Foam-Enhanced Devolatilization of Polystyrene Melt in a Vented Extruder

Alexander Tukachinsky, Yeshayahu Talmon, and Zehev Tadmor
Dept. of Chemical Engineering, Technion, Israel Institute of Technology, Haifa 32000, Israel

Vented extruder devolatilization (DV) of PS melt containing 6,000 ppm styrene was studied by scanning electron microscopy (SEM) and video photography. Vacuum DV of a polymer is accompanied by foaming, which starts instantaneously upon supersaturation of the stretched melt and is enhanced at higher speeds of the vented extruder screw. As the volatiles are removed from the melt, foaming gradually ceases, starting with the pushing flight of the screw. The experimental installation design allowed us to quench the polymer melt in the DV zone at various stages of the process. Samples taken from four areas of the channel width were investigated by SEM. Bubble nucleation in the melt appears to take place mainly in the border area adjoining the gas phase. In the shear field caused by screw rotation, large bubbles become noticeably elongated. Their surface, as well as the free surface of the melt, is covered with blisters, 1–100 μm in size. Microblisters are often concentrated in areas subjected to stretching. Calculations of cooling due to volatile evaporation and of heating due to viscous dissipation near a growing bubble shows that the process of foam-enhanced DV of a PS/styrene system can be regarded isothermal if the initial volatile concentration does not exceed approximately 1%.

Introduction

The removal of residual volatiles, such as unreacted monomers, solvents and other low molecular weight components from polymeric melts, is a post-reactor processing step needed to improve properties, recover material, or meet environmental or health requirements. This operation, devolatilization (DV), is carried out by exposing the melt to vacuum in specially designed equipment, or devolatilizers (DVRs). These can be subdivided into two broad categories: falling-strand DVRs, in which the melt is extruded into thin strands that fall gravitationally in a vacuum tank, and rotating type DVRs such as vented extruders, in which a rotating melt pool and recycling film are exposed to vacuum (Biesenberger and Sebastian, 1983). A vented single screw DVR is basically similar to a regular extruder, but for a screw profile that ensures a partially filled channel in a given section of the extruder.

With low initial volatile content, foaming is a positive phenomenon because it increases the rate of DV (Lee and Biesenberger, 1989). However, the tendency to foam decreases with decreasing volatile content. Some experimental data indicate that bubble nucleation, which leads to foaming, is enhanced by mechanical stresses (Han and Han, 1988; Lee, 1991). In this respect, a vented extruder is superior to falling strand DVRs, because the polymer melt is continuously subjected to shear stresses in the extruder. Moreover, agitation of the material takes place within the screw channel; thus, free surfaces are continuously renewed, leading to increased DV rates. Shear stresses cause stretching of the bubbles, and affect the processes of bubble growth, coalescence, and burst.

Existing theories of DV in rotating DVRs are based on macroscopic observations (Lee and Biesenberger, 1989; Foster and Lindt, 1990). But to fully understand the mechanism of polymer melt foam-enhanced DV in a vented extruder, including bubble nucleation, growth and burst, it is necessary to study experimentally the microstructure of a melt throughout the process. Albalak et al. (1990) used scanning electron microscopy (SEM) to study falling-strand DV. Specimens for SEM were obtained by water quenching of melted strands. It was shown that falling-strand DV is accomplished by a complex bubble transport mechanism: the free surface of the melt and

Correspondence concerning this article should be addressed to Y. Talmon.

the inner surface of large voids are covered with tiny blisters (about 1 to 100 μm in size) which burst and release the volatiles into the ambient space or into macrobubbles. A new generation of blisters is then formed, and so on, until volatile concentration in the polymer drops below superheating levels.

In the present work, the above-mentioned experimental technique of melt quenching and consequent SEM investigation is applied to elucidate microstructural effects in the process, to gain better understanding of rolling-pool-and-film DV, with emphasis on the role played by shear.

Experimental

The experimental system consists of two single-screw extruders connected in series (Figure 1). Each extruder has an independent drive, with controlled rpm. The first extruder (20 mm diameter) is used for polymer melting and homogenizing. The second one (50 mm diameter) is the vented extruder. Polymer melt is fed from the first extruder into the second extruder. A sampling port in the barrel of the vented extruder is located three leads downstream from the melt inlet. The port is used for venting gases, for observation, for quenching and for polymer sampling. A three-way nozzle is installed on the port. Its central arm, the widest one, is covered with glass, and serves for observing the melt during DV. Vacuum venting is carried out via another arm of the nozzle. Cold water for quenching the melt is fed through the third arm. Solenoid valves are installed on the second and the third arms of the nozzle. They are regulated by an automatic control system, that opens or closes the valves at predetermined times, and stops the screw of the vented extruder simultaneously. A magnet transducer of screw angular position is used to stop the screw in a position convenient for sampling.

The vacuum system is made of a vacuum pump, a 100 L vacuum buffer tank, a vacuum trap and a gauge. To prevent contamination of the polymer specimens, cold water for quenching is run in a filtered closed cycle.

Electric heaters control the temperature of both extruders in eight independent control zones. The temperature of DV zone in the series of experiments described here was 235°C, the absolute pressure in the system during DV was 3 mm Hg, the polymer flow rate was 0.54 kg/h, the screw speed of the vented extruder was 72 and 20 rpm, and the corresponding shear rates in screw channel were 94 and 26 s^{-1}.

The material used was commercial polystyrene (HH 102E, by the Israeli Petrochemical Enterprises) enriched with styrene to 6,000 ppm. This was done by placing PS pellets in a closed vessel saturated with styrene vapors. The samples of enriched PS, dissolved in dichloromethane, were analyzed for styrene content by gas chromatography.

Procedure

Both extruders were heated and brought to steady-state conditions. Styrene-enriched PS pellets were fed by a vibrofeeder into the hopper of the first extruder. This way the vibrofeeder controlled the flow rate throughout the system. The melted and homogenized material was fed into the second extruder, at ambient pressure in the initial stage of the experiment. Screw speed of the vented extruder was set to a high enough value (20 to 72 rpm) to prevent complete filling of the screw channel

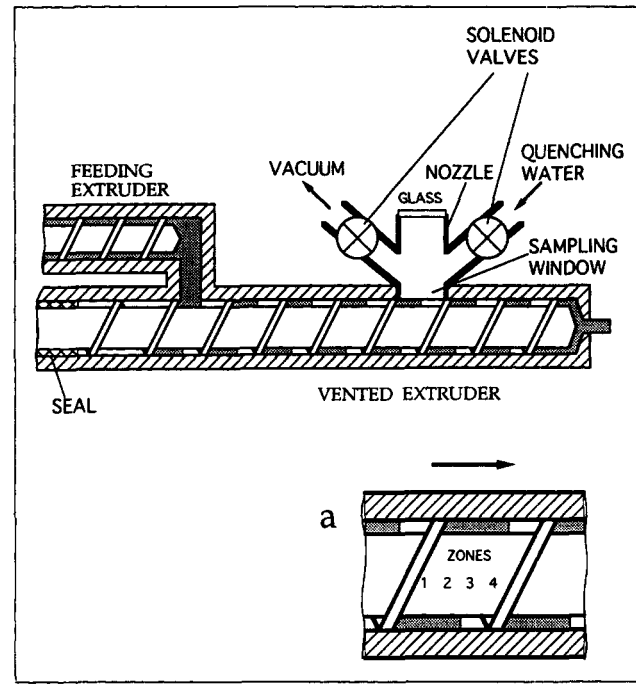

Figure 1. Experimental installation.

(a) Is the four zones of melt sampling along with width of screw channel. Arrow points the direction of melt movement in the extruder.

along its length, with the exception of a short section before the outlet die.

The vacuum pump maintained a required level of vacuum in the buffer tank. The water pump provided the pressure in the water feeding system for quenching. Both solenoid valves were closed at the start. At a certain moment, the automatic control system opened first the valve connecting the vacuum tank with the inner space of the vented extruder, to start DV. After a certain predetermined time lapse (0.5 to 20 s), the automatic system opened the second valve to feed quenching water, and, simultaneously, the vented extruder screw was stopped. The screw angular position transducer assured that every time the screw stopped, its interflight space (from flight to flight) was facing the sampling port. The first volume of waste cooling water from the sampling zone got into the buffer tank; then, the flow of water was directed into a container in the closed cooling system, until completely cooling the extruder. The three-arm nozzle was then dismantled.

The inner space of the extruder was dried, and polymer samples were taken after flooding the sampling port with liquid nitrogen. Polymer chips were chopped off the four zones of the screw channel width (Figure 1a). The first zone is located directly in front of the pushing flight, the second and the third ones in the middle part of the interflight space, and the fourth zone behind the rear edge of the following flight. The collected polymer chips were immersed again in liquid nitrogen and fractured into specimens about 5 mm in size. Specimen thickness was determined by the thickness of the melt layer on the screw, and did not exceed the screw channel height of 2 mm. The specimens were cemented to metal specimen stubs, and sputter-coated with a 25 nm gold layer. They were examined in a JEOL T-300 scanning electron microscope, in the sec-

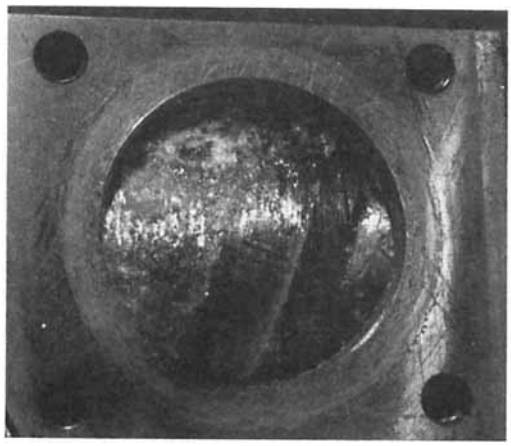

Figure 2. Sampling port with the polymer quenched after 10 s vacuum exposure.

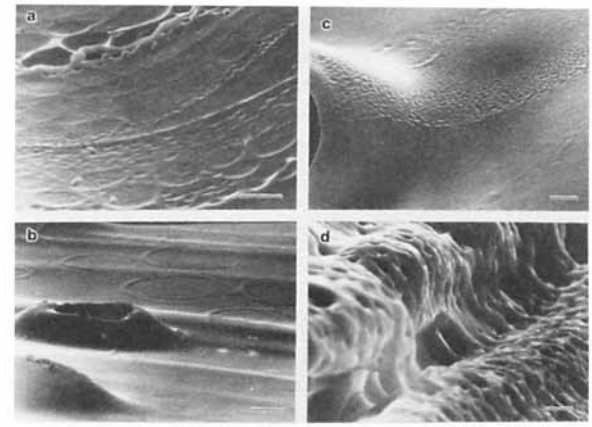

Figure 3. Scanning electron micrographs of quenched polystyrene specimens (screw speed of 72 rpm, *t* is vacuum treatment time, *n* is number of the zone).

(a) Blister traces on the free surface ($t = 0.8$ s, $n = 4$, bar = 5 μm); (b) macrocraters and big blister traces ($t = 0.5$ s, $n = 4$, bar = 100 μm); (c) microblister traces near a macrocrater ($t = 0.5$ s, $n = 1$, bar = 10 μm); (d) micropores on the macrobubble surface ($t = 0.8$ s, $n = 2$, bar = 10 μm).

ondary electron imaging mode at an acceleration voltage of 25 kV and at original magnifications up to 20,000 X.

Polymer melt foaming in the vented extruder was also recorded by a video camera. For this the sampling window was covered with a Pyrex glass and sealed. Volatiles were pumped off through another port in the vented extruder barrel. A Sony video-camcorder CCD-F450E was mounted above the window, and the shutter speed was up to 4,000 s^{-1}. The camera field of view covered the entire window (40 mm diameter), a little less than one lead of the screw (50 mm). Shooting was started about half a minute before vacuum was applied within DV zone, and continued for 2 to 3 minutes, when steady-state vented extrusion conditions were attained.

Results

Melt foaming starts, according to the video footage as well as to microphotographs, the instant the vacuum is applied. The kinetics of foaming is strongly dependent on the speed of the screw. At 72 rpm, the strongest foaming occurs during the first 5 seconds: the melt actually turns into foam, filling the whole width of the screw channel. Then foaming subsides, and by the fifth second, a strip of nonfoamed melt appears in the zone adjacent to the pushing surface of the flight (Figure 2). The strip, about 7 mm wide and divided by quite a distinct border from the rest of the foamed mass, was observed during the subsequent 15–20 s. In about half a minute after the vacuum had been applied, foaming terminated throughout the observed space. Thus, under steady-state conditions, polymer melt foaming takes place only in the starting section of the screw in no more than two leads of its length.

In experiments at lower screw rotation speed (20 rpm), similar phenomena were observed, but on a different time scale. Intensive foaming developed during one to two seconds after vacuum was applied, and continued for about 15 s. At the end of that period, a strip of nonfoamed melt was formed near the screw flight; foaming receded and then ended in about 1 minute from the beginning of the process.

Scanning electron micrographs of quenched specimens of a foamed polymer melt show microstructural features similar to those observed by Albalak et al. (1990) in their studies of falling-strand DV. We found the free surface of the material and the surface of macrobubbles covered in some sites by traces of micro and miniblisters, about 1 to 100 μm in size (Figure 3a). The size and frequency of appearance of such areas depend on duration of vacuum exposure and on the particular zone of the screw channel (as was mentioned above, the channel width was subdivided into four zones). Foaming developed considerably faster than in falling-strand DV under similar conditions, where 10 seconds were needed for complete foaming of the strand core (Tadmor et al., 1992).

When the screw speed was 72 rpm, the following times of vacuum exposure (prior to quenching) were chosen: 0.5, 0.8, 1.0, 2.0, 5.0, 10 and 20 seconds. Already at 0.5 s, single macrocraters of two types were observed (Figure 3b); also, microblister traces were found in the first and fourth zones of the channel (Figure 3c). At $t = 0.8$ s (one rotation of the screw), the material was fully foamed, both at macro- and microlevel. Micro- and miniblisters covered the entire outer surface of specimens and inner surface of macrobubbles (Figures 3a and 3d). Similar images of vigorous foaming were also observed at $t = 1$ s and $t = 2$ s. At $t = 5$ s, an essentially different picture was observed. Bubbles were absent from the first zone (adjacent to the pushing flight). In the three remaining zones, traces of blisters were seen as before, but they were not dispersed so densely; they were mainly located on the inner surface of the pores remaining from macrobubbles (Figure 4a). After 10 seconds had elapsed, there were still many macrobubbles in zones 2, 3, and 4, but notably less fresh traces of microblisters were seen. At $t = 20$ s, foaming on macrolevel was not observed in any of the four zones.

Shear is the main difference between foaming in a vented extruder and foaming during falling-strand DV. Macrobubbles (100 μm and bigger) became oblong. The ratio of a bubble length in the direction of shear to its width reached 10 and

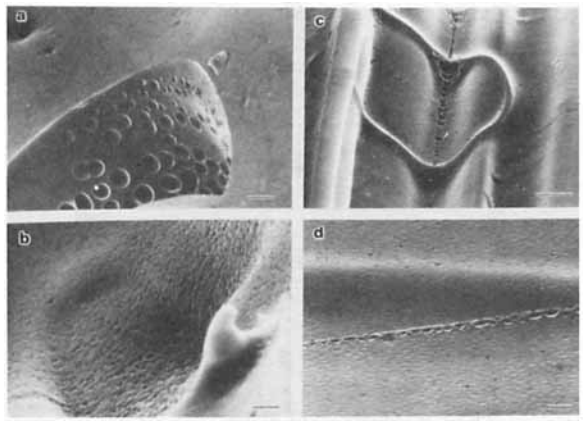

Figure 4. Scanning electron micrographs of quenched polystyrene specimens (screw speed of 72 rpm, *t* is vacuum treatment time, *n* is number of the zone).

(a) Microblister traces on the macropore surface ($t = 5$ s, $n = 4$, bar = 10 μm); (b) surface covered with micropores ($t = 2$ s, $n = 2$, bar = 10 μm); (c) blister chain in a gully ($t = 1$ s, $n = 4$, bar = 10 μm); (d) blister chain ($t = 20$ s, $n = 4$, bar = 10 μm).

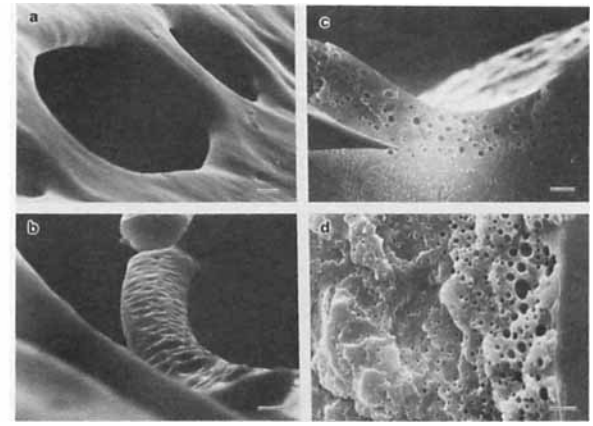

Figure 6. Scanning electron micrographs of quenched polystyrene specimens (screw speed is 72 rpm, *t* is vacuum treatment time, *n* is number of the zone).

(a) Coalescing microbubbles ($t = 0.8$ s, $n = 2$, bar = 1 μm); (b) blister traces at the stretched neck between coalescing bubbles ($t = 0.8$ s, $n = 3$, bar = 10 μm); (c, d) microbubbles on the cross section near free surface ($t = 1$ s, $n = 2$, bar = 10 μm).

more. The shape of smaller microbubbles (< 10 μm) remained closer to spherical.

Blisters were mostly located on the surface of the material in groups of various sizes and shapes: a very large group covering a significant part of a specimen surface (Figure 4b), or chains of blisters either following (Figure 4c) or not following (Figure 4d) lines of surface deformation. Quite often the remaining rim of a partially reabsorbed big blister served as a border of a blister-covered patch (Figure 5). "Bridges," formed as a result of coalescence of neighboring bubbles (Figure 6a), were also found to be the sites of microblister concentration (Figure 6b). Microbubbles the size of microns were not frequently observed in the bulk of the polymer. When they were found, they were located near the surface (Figure 6c); their size increased the closer they were to the surface (Figure 6d).

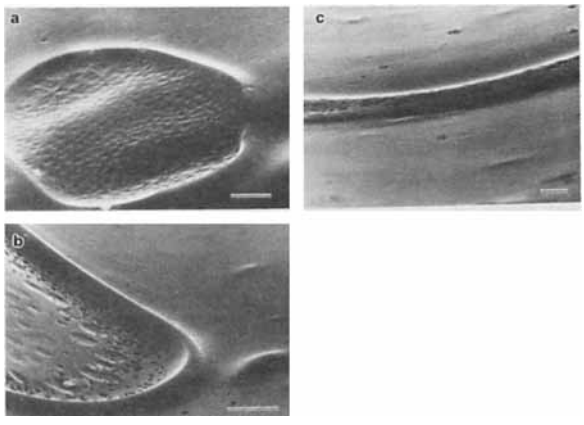

Figure 5. Scanning electron micrographs of quenched polystyrene specimens (screw speed is 72 rpm, *t* is vacuum treatment time, *n* is number of the zone).

(a) Microblisters cover the surface inside a big blister trace ($t = 2$ s, $n = 3$, bar = 10 μm); (b) microblister traces near a big blister trace ($t = 1$ s, $n = 3$, bar = 5 μm); (c) microblister traces upon a big blister trace ($t = 1$ s, $n = 3$, bar = 1 μm).

Discussion

When a polymer melt in a DV extruder enters the vented zone, it becomes supersaturated due to a sudden decrease of ambient pressure. In our experiments, the time count up to quenching starts at the moment of the prompt exposure to vacuum in the inner space of the vented extruder, all along the length of the partially filled screw. Melt sampling at different times but in the same place, closely simulates sampling along the length of a vented extruder working in steady-state conditions. Strictly speaking, that is true only for a limited time, when fresh material, which enters the vented extruder after vacuum set-on, has not yet reached the sampling window. That time can be estimated from standard assumptions, namely, laminar flow of the melt, and the melt sticking to the surface of the screw and the barrel. At 72 rpm, the shortest time for the first particles of the fresh material to reach the sampling window (situated three leads downstream from the inlet) is 3.6 s; half-time of the material renewal is 7.2 s. At 20 rpm, the corresponding times are 9 and 18 s. This should be taken into account in the interpretation of the results.

The transverse pressure gradient induced by drag flow in the screw channel, dp/dx, is the cause to the appearance of a strip of nonfoamed material at the pushing screw flight. At the beginning of vigorous foaming this strip is absent. But, as foaming subsides, viscous resistance creates cross channel pressure at the pushing flight, sufficient to suppress foaming.

When viscosity is constant, we have (Tadmor and Gogos, 1979):

$$\frac{dp}{dx}=6\eta\frac{V_{bx}}{H^2}=6\eta\frac{\pi ND\sin\theta}{H^2} \qquad (1)$$

where x is the coordinate normal to screw flight, V_{bx} is the component of screw flight velocity in the direction x, H is channel depth, N is frequency of screw rotation, and θ is screw helix angle.

At our experimental conditions, at rpm = 72 we obtain $dp/dx = 42.4$ MPa/m. For a melt strip 7 mm wide, the pressure before the pushing flight will be 0.3 MPa (about 3 atmospheres). At that stage, DV can take place only near the free surface of the pool.

After reaching steady-state, foaming of the material under the sampling window is no longer observed. Thus, foaming is completed upstream of the window within three screw turns, that is within less than 3.6 at 72 rpm and within 9 s at 20 rpm. Hence, as was mentioned above, the foaming process in a vented extruder is more intensive and rapid compared to falling-strand DV. The process becomes more intensive with increasing screw speed. This is probably due to the effect of shear and material mixing at all stages of foaming, namely, bubble nucleation, growth, coalescence, and burst.

Classical nucleation theory (Blander and Katz, 1975) does not predict the influence of simple shear on nucleation rate, because the isotropic part of the stress tensor (pressure) does not change. In a polymer melt, shear may cause increase of pressure, due to the effect of normal stresses and thus suppress cavitation. At the same time, complex microflows develop during melt foaming in a vented extruder, causing three-dimensional stretching of the material at some places, such as at the base of the thin membrane between two growing bubbles. This leads to negative pressures, which in turn brings about an increase in supersaturation and consequent lowering of the critical work for bubble nucleation:

$$W_{cr}=\frac{16\pi\sigma^3}{3(p_v-p_m)^2}, \qquad (2)$$

σ is the surface tension, p_m is pressure in the melt, and p_v is pressure of volatiles in the bubble (close to equilibrium vapor pressure p_s at given volatile concentration and temperature). Nucleation rate is proportional to $\exp(-W_{cr}/kT)$; it becomes higher as W_{cr} decreases.

One characteristic phenomenon observed during SEM studies of our specimens is microbubble formation near the edge of a big blister (Figures 5b and 5c). Stretching stresses, S, that develop on the polymer surface near the shell of a growing blister (Figure 7), can be estimated by assuming the volatile pressure within the blister to be equal to the equilibrium vapor pressure, p_s:

$$S=0.25\,(p_s-p)\,d/h, \qquad (3)$$

where d is the blister diameter, h is the shell thickness, and p is the outer pressure. The rims of the macroblisters on Figures 5b and 5c have the following dimensions: $d\approx 50$ μm and $h\approx 1$ μm. Equilibrium vapor pressure in the styrene/polystyrene system at 235°C and at styrene concentration of 6,000 ppm, is $p_s = 1.4\times 10^4$ Pa (Biesenberger and Sebastian, 1983); the absolute pressure in the extruder is $p = 400$ Pa. Based on that we obtain $S = 1.7\times 10^5$ Pa. Such stretching stress can undoubtedly facilitate bubble nucleation.

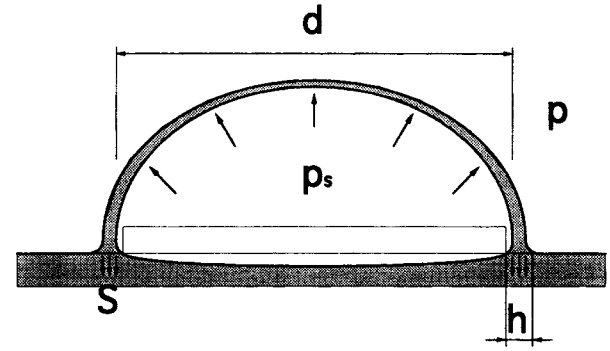

Figure 7. Cross section of a blister on the surface of the melt.

Scheme for calculation of stresses.

If the growing blister is assumed to be a hemisphere, and its base is moving on the melt surface during its growth like a widening ring, then all the surfaces underlying the blister are subjected to stretching. That may explain the frequently observed effect of microblisters covering the surface of the remains of a big blister (Figure 5a). In that case nucleation takes place only in the surface layer of the polymer melt. Also, negative pressures most probably cause concentration of blisters at stretched necks between coalescing bubbles (Figure 6b).

Negative pressures are especially important in a melt that has already undergone partial DV, and thus has low volatile content. For a bubble to grow, its radius must be more than the critical value $R_{cr}=2\sigma/(p_v-p_m)$. Assuming the vapor pressure in a nucleus is the equilibrium saturation pressure $p_v=p_s$, we obtain $R_{cr}=3.7$ μm for our experimental conditions, at styrene concentration $w=6{,}000$ ppm. When, however, w has been reduced to 500 ppm, $R_{cr}\approx 50$ μm, and nucleation is suppressed. When p_m becomes negative, to values about -10^5 Pa (see the calculation above), the critical radius of a bubble is about 0.5 μm, irrespective of the residual styrene concentration.

In our experiments, traces of microblisters on a specimen surface, fixed by quenching, usually have the size of one to several micrometers. In the areas of stretching, smaller traces are observed, too (Figures 5b and 5c). This size is approximately equal to the critical size of a bubble. Thus, it appears that microblisters are in fact bubbles that had nucleated in the immediate vicinity of a melt surface, and burst almost immediately without growing.

In the foregoing discussion isothermal conditions were assumed. However, thermal effects due to volatile evaporation and viscous dissipation may be significant in melt DV. Therefore, the magnitude of these effects is assessed. Analysis of this problem and detailed calculations are given by Tukachinsky (1993). The main results of these calculations are: (a) cooling due to volatile evaporation in the course of flash DV is significant only if the residual concentration of the volatiles is at least a few percent, certainly higher than the styrene concentration in our experiments; (b) the upper limit of the heating rate due to viscous dissipation is $dT/dt\approx 2$°C, and thus negligible in our case; (c) no appreciable heat is generated at

the surface of the growing bubble in the melt at our experimental conditions.

The small temperature rise due to viscous dissipation is insufficient to cause vigorous nucleation of blisters near the surface of a growing bubble. As microblisters are formed not only on the surface of macrobubbles, but in general on free surface of the melt, one may assume that the critical work of bubble nucleation near the surface is lower than in the bulk of the liquid. Indeed, the dynamics of nucleation process in a highly viscous medium may be determined not only by surface tension, but also by viscosity. That the quantity of liquid to be "moved apart" is less (and so the viscous resistance to be overcome is less) may turn out to be decisive in the process of blister nucleation.

Finally, a comment concerning the efficiency of volatile removal by foaming. Volatile volume in the gas phase is much larger than the volume the volatile occupies when dissolved in the polymer. Calculation shows that the material which has been thoroughly devolatilized is located in a thin layer near the surface of the bubble containing volatile vapor. For the PS/styrene system and for our experimental conditions (235°C, $w = 6{,}000$ ppm, $p = 400$ Pa), the thickness of that layer is about $0.03R$ at the initial stage of bubble growth, and about one-thousandth of the transverse size of a grown bubble, whether spherical or oblong. Foaming has obviously significant effect on DV rate only if the melt turns into low-density foam, with thin partitions between the cells.

Conclusions

DV of the polystyrene/styrene system in a vented extruder is accompanied by foaming and blistering. During their growth in a shear field, the bubbles become considerably elongated; this facilitates mass transfer. Vigorous foaming begins earlier and ends sooner than during falling-strand DV under similar conditions. With increasing screw speed, the foaming time becomes shorter. Cessation of the foaming starts at the screw pushing flight and spreads forward through the entire polymer volume.

Bubble nucleation takes place mostly close to the free surface of the melt and in the vicinity of macrobubble surface. Microblisters are often situated randomly on the surface; their concentration is higher in areas of elongational microflows, where stretching stresses increase the degree of supersaturation.

According to theoretical assessment, neither volatile evaporation, nor viscous dissipation near a growing bubble cause considerable change in the temperature of the material, unless styrene initial concentration in the system exceeds 1%.

Acknowledgment

This research was supported in part by the German-Israeli Foundation for Scientific Research and Development (GIF). We thank Ms. Judith Schmidt and Ms. Bertha Shdemati for expert technical help.

Notation

h = thickness
H = screw channel depth
k = Boltzman's constant
n = number of the zone across screw channel
p_s = saturation pressure
R = bubble radius
R_0 = initial bubble radius
R_{cr} = critical bubble radius
t = time
T = temperature
V = bubble volume
w = volatile concentration
W_{cr} = critical work of bubble nucleation
x = Cartesian coordinates

Greek letter

η = melt viscosity

Literature Cited

Albalak, R. J., Z. Tadmor, and Y. Talmon, "Polymer Melt Devolatilization Mechanisms," *AIChE J.*, **36**, 1313 (1990).

Amon, M., and C. D. Denson, "A Study of the Dynamics of Foam Growth: Analysis of the Growth of Closely Spaced Spherical Bubbles," *Polym. Eng. Sci.*, **24**, 1026 (1984).

Biesenberger, J. A., and D. H. Sebastian, *Principles of Polymerization Engineering*, Wiley-Interscience, New York (1983).

Bird, R. B., W. E. Stewart, and E. N. Lightfoot, *Transport Phenomena*, Wiley, New York (1960).

Blander, M., and I. L. Katz, "Bubble Nucleation in Liquids," *AIChE J.*, **21**, 833 (1975).

Foster, R. W., and J. T. Lindt, "Twin Screw Extrusion Devolatilization: From Foam to Bubble Free Mass Transfer," *Polym. Eng. Sci.*, **30**, 621 (1990).

Han, I. H., and C. D. Han, "A Study of Bubble Nucleation in a Mixture of Molten Polymer and Volatile Liquid in a Shear Flow Field," *Polym. Eng. Sci.*, **28**, 1616 (1988).

Lee, S. T., and J. A. Biesenberger, "A Fundamental Study of Polymer Melt Devolatilization. IV. Some Theories and Models for Foam-Enhanced Devolatilization," *Polym. Eng. Sci.*, **29**, 782 (1989).

Lee, S. T., "Shear Effects on Thermoplastic Foam Nucleation," 49th SPE ANTEC Preps. (1991).

Tadmor, Z., and C. G. Gogos, *Principles of Polymer Processing*, Wiley, New York (1979).

Tadmor, Z., Y. Talmon, and H. D. Fritz, "Polymer Melt Devolatilization," Final Report, GIF Project Nr. I 0060-277.06/87 (1992).

Tukachinsky, A., "Effect of Acoustic Waves and Shear on Polymer Melt Devolatilization," D.Sc. Diss., Technion, Israel (1993).

Manuscript received Dec. 21, 1992, and revision received July 6, 1993.